

Conjoined Lorenz twins—a new pseudohyperbolic attractor in three-dimensional maps and flows

Cite as: Chaos 32, 121107 (2022); <https://doi.org/10.1063/5.0123426>

Submitted: 30 August 2022 • Accepted: 05 December 2022 • Published Online: 21 December 2022

 Sergey Gonchenko,  Efrosiniia Karatetskaia,  Alexey Kazakov, et al.



[View Online](#)



[Export Citation](#)



[CrossMark](#)



Chaos

Special Topic: Nonlinear Model
Reduction From Equations and Data

Submit Today!

Conjoined Lorenz twins—a new pseudohyperbolic attractor in three-dimensional maps and flows

Cite as: Chaos 32, 121107 (2022); doi: 10.1063/5.0123426

Submitted: 30 August 2022 · Accepted: 5 December 2022 ·

Published Online: 21 December 2022



View Online



Export Citation



CrossMark

Sergey Gonchenko,^{1,2,a)}  Efrosiniia Karatetskaia,^{2,b)}  Alexey Kazakov,^{1,2,c)}  and Vyacheslav Kruglov^{3,d)} 

AFFILIATIONS

¹Scientific and Educational Mathematical Center “Mathematics of Future Technologies,” Lobachevsky State University of Nizhny Novgorod, 23 Gagarina Ave., 603950 Nizhny Novgorod, Russia

²Laboratory of Dynamical Systems and Applications, National Research University Higher School of Economics, 25/12 Bolshaya Pecherskaya Ulitsa, 603155 Nizhny Novgorod, Russia

³Kotelnikov’s Institute of Radio-Engineering and Electronics of RAS, Saratov Branch, Zelenaya 38, Saratov 410019, Russia

^{a)}Electronic mail: sergey.gonchenko@mail.ru

^{b)}Electronic mail: eyukaratetskaya@gmail.com

^{c)}Author to whom correspondence should be addressed: kazakovdz@yandex.ru

^{d)}Electronic mail: kruglovyacheslav@gmail.com

ABSTRACT

We describe new types of Lorenz-like attractors for three-dimensional flows and maps with symmetries. We give an example of a three-dimensional system of differential equations, which is centrally symmetric and mirror symmetric. We show that the system has a Lorenz-like attractor, which contains three saddle equilibrium states and consists of two mirror-symmetric components that are adjacent at the symmetry plane. We also found a discrete-time analog of this “conjoined-twins” attractor in a cubic three-dimensional Hénon map with a central symmetry. We show numerically that both attractors are pseudohyperbolic, which guarantees that each orbit of the attractor has a positive maximal Lyapunov exponent, and this property is preserved under small perturbations. We also describe bifurcation scenarios for the emergence of the attractors in one-parameter families of three-dimensional flows and maps possessing the symmetries.

Published under an exclusive license by AIP Publishing. <https://doi.org/10.1063/5.0123426>

One of the most fundamental problems in multidimensional chaos theory is the study of strange attractors, which are robustly chaotic (i.e., they remain chaotic after small perturbations of the system). It was hypothesized in Ref. 1 that the robustness of chaoticity is equivalent to the pseudohyperbolicity of the attractor. Pseudohyperbolicity is a generalization of hyperbolicity. The main characteristic property of a pseudohyperbolic attractor is that each of its orbits has a positive maximal Lyapunov exponent. In addition, this property must be preserved under small perturbations. The foundations of the theory of pseudohyperbolic attractors were laid by Turaev and Shilnikov, who showed that the class of pseudohyperbolic attractors, besides the classical Lorenz and hyperbolic attractors, also includes wild attractors, which contain orbits of homoclinic tangencies. They also gave the first examples of wild pseudohyperbolic attractors. By now, several wild (structurally unstable) pseudohyperbolic attractors have been found: Lorenz-like and heteroclinic Lorenz-like attractors in 3D Hénon-like maps,^{2,3} discrete Lorenz-like attractors in the model of Celtic stone,⁴ the figure-8 attractor in the Chaplygin

top model,⁵ and the wild spiral attractor in a four-dimensional extension of the Lorenz model.¹ In this paper, we present a new example of a wild pseudohyperbolic attractor—the so-called conjoined Lorenz twins, found in a 3D Hénon-like map with a central symmetry. We also describe a similar type of Lorenz attractor in a 3D system of ordinary differential equations; this new type of Lorenz attractor contains three saddle equilibria. We demonstrate that such attractors naturally appear in systems with symmetries and describe universal bifurcation mechanisms that lead to these attractors. To establish the chaoticity of these attractors, we employ numerical methods, which are explicitly based on the verification of the pseudohyperbolicity conditions from Refs. 6 and 7.

I. INTRODUCTION

For uniformly hyperbolic and Lorenz attractors, their chaoticity does not disappear at small perturbations; therefore, they can

be classified as genuinely strange attractors with certainty. Classical examples of nontrivial hyperbolic attractors are well known: these are the Smale–Williams solenoid and its generalizations,^{8–10} the Anosov and DA-attractors,⁸ and the Plykin attractor.^{11,12} Examples of physically relevant systems that exhibit uniformly hyperbolic chaos were discovered and studied by Kuznetsov and his colleagues;^{13–15} see a comprehensive survey in the book.¹⁶

Unlike the hyperbolic attractors, the Lorenz attractor was found, from the very beginning, in an applied problem. A mathematical theory for this class of attractors was built later by Afraimovich–Bykov–Shilnikov, Guckenheimer–Williams, and others.^{17–28} Computer-assisted proof of robust chaoticity of the strange attractor in the classical Lorenz model itself was given by Tucker.²⁹ The study of Lorenz attractors and their generalizations remains still relevant, and a series of papers has been published on this topic in recent years; see, e.g., Refs. 30–36.

Both Lorenz attractors and uniformly hyperbolic attractors belong to a more general class of pseudohyperbolic attractors.⁶ Their common property is the existence of a continuous invariant splitting of the tangent space in a neighborhood of an attractor into a direct sum of two linear subspaces E^{ss} and E^{cu} : the linearized system restricted to E^{ss} is uniformly contracting, whereas in E^{cu} , it uniformly expands volumes. In the case of hyperbolic attractors, the field of subspaces E^{cu} is given by tangents to the unstable manifolds. In the general pseudohyperbolic case, the linearized system can contract certain directions in E^{cu} ; however, the total volume expansion in E^{cu} ensures that the maximal Lyapunov exponent for every trajectory of the attractor is always positive. Crucially, any possible contraction in E^{cu} must be weaker than the contraction in E^{ss} —this guarantees that both the positivity of the maximal Lyapunov exponent and the whole pseudohyperbolic structure are preserved at small perturbations of the system.

The Lorenz attractor is the most known example of a pseudohyperbolic attractor. It is not uniformly hyperbolic and is not structurally stable,^{19,37} although all its periodic orbits are saddle and their invariant manifolds intersect transversally. These are common properties for a wider class of singular hyperbolic attractors.^{27,28}

As it was shown in Ref. 6, the class of pseudohyperbolic attractors is not exhausted by hyperbolic and singular hyperbolic attractors, and there also exist the so-called *wild pseudohyperbolic attractors*. Such attractors admit homoclinic and heteroclinic tangencies between saddle periodic orbits, and such tangencies exist for a dense set of parameter values. Thus, systems with wild pseudohyperbolic attractors belong to the so-called Newhouse domain,³⁸ all systems from which possess wild hyperbolic sets whose stable and unstable manifolds have persistent (unremovable) tangencies. This leads to ultimately rich and complicated dynamics,^{39–41} a complete description of which is impossible as is proved in Ref. 42. An example of a four-dimensional extension of the Lorenz system, which contains the Turaev–Shilnikov wild attractor, was found in Ref. 1.

Except for this attractor and two other examples (figure-8 attractor of Ref. 5 and the “heteroclinic” attractor in Ref. 3), all the other known examples of wild pseudohyperbolic attractors belong to the class of *discrete Lorenz-like* attractors. The shape of these attractors is similar to the Lorenz homoclinic butterfly, but they appear in discrete-time dynamical systems (3D maps). More formally, we define a *discrete Lorenz-like attractor* \mathcal{A} of a three-dimensional map

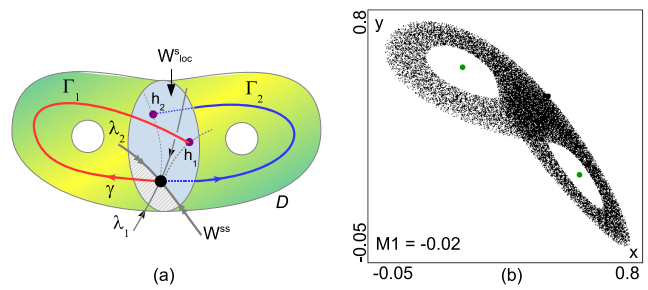


FIG. 1. (a) Skeleton-scheme for the discrete Lorenz attractor: D is an adsorbing domain (a solid pretzel); the curves $\Gamma_i \cup [h_i, O]$ are non-contractible in D ; homoclinic points h_1 and h_2 reside in the same part of $W_{loc}^{ss} \setminus W^{ss}$. (b) The (x, y) -projection of the phase portrait of the discrete Lorenz attractor for the three-dimensional Hénon map $\bar{x} = y, \bar{y} = z, \bar{z} = M_1 + Bx + M_2y - z^2$, where $B = 0.7, M_1 = -0.02, M_2 = 0.85$; from Ref. 3.

as follows (cf. Ref. 3):

- (i) \mathcal{A} contains a saddle fixed point O with eigenvalues $\gamma, \lambda_1, \lambda_2$ such that $|\gamma| > 1, 0 < |\lambda_2| < \lambda_1 < 1, |\lambda_1\gamma| > 1$, and $|\lambda_1\lambda_2\gamma| < 1$, and it does not contain other fixed points;
- (ii) an adsorbing domain D of \mathcal{A} has a pretzel shape (a ball with two handles);
- (iii) \mathcal{A} contains the unstable separatrices Γ_1 and Γ_2 (connected components of the set $W^u(O) \setminus O$);
- (iv) Γ_1 leaves O and passes along one handle of the pretzel D and Γ_2 along the other handle; and
- (v) all the homoclinic points of the intersections $\Gamma_1 \cap W_{loc}^{ss}(O)$ and $\Gamma_2 \cap W_{loc}^{ss}(O)$ belong to the same half of $W_{loc}^{ss}(O) \setminus W^{ss}(O)$; see Fig. 1(a).

The first example of such an attractor was given in Ref. 43 for the case of a quadratic three-dimensional Hénon map; see Fig. 1(b). The important theoretical result on this topic was obtained in Ref. 7, where, in particular, it was shown that the Poincaré map of a periodically perturbed 3D system with the Lorenz attractor can have a wild pseudohyperbolic discrete Lorenz-like attractor when this perturbation is sufficiently small. The theory of discrete Lorenz-like attractors was further developed in a number of papers; see, e.g., Refs. 3, 31, and 44–46.

In the present paper, we report new examples of Lorenz-like attractors for three-dimensional maps and flows; see Fig. 2. We call them “*conjoined Lorenz twins*”. The search for such attractors was motivated by Ref. 3, where it was conjectured (in Remark 4 there) that a three-dimensional map can have an analog of a discrete Lorenz-like attractor containing a fixed point and an orbit of period two.

Here, we found such an attractor [see Fig. 2(a)] in the centrally symmetric cubic Hénon map,

$$\begin{cases} \bar{x} = y, \\ \bar{y} = z, \\ \bar{z} = Bx + Cy + Az - \frac{3}{2}zy^2 + 2z^3 \end{cases} \quad (1)$$

for some regions of parameter values A, B , and C .

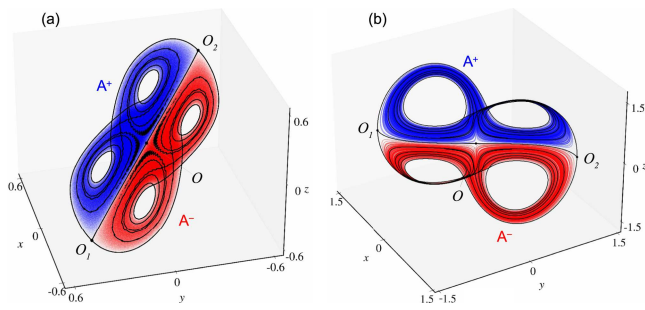


FIG. 2. Conjoined Lorenz twins: (a) in the 3D map (1) for $(A, B, C) = (-0.9, 0.7, 0.9)$; here, the attractor contains the central saddle fixed point O and the period-2 saddle orbit (O_1, O_2) ; (b) in the 3D flow (2) for $(\alpha, \lambda) = (0.4, -0.15)$, here, the attractor contains the saddle equilibria $O, O_1,$ and O_2 . These attractors consist of two halves A^+ and A^- (colored in blue and red, respectively). The half-attractors A^+ and A^- are obtained by iterations of the initial points taken on opposite sides of a two-dimensional plane containing the line $[O_1, O, O_2]$. The pieces of the unstable separatrices $W^u(O)$ and $W^u(O_i)$ are also plotted. Each half-attractor contains three points $O, O_1,$ and O_2 .

We also found a continuous-time analog [see Fig. 2(b)] in the following system of differential equations, which is both centrally and mirror symmetric:

$$\begin{cases} \dot{x} = -x + y, \\ \dot{y} = -\lambda y + (1 - y^2 - z^2)x, \\ \dot{z} = -\alpha z + 2xyz, \end{cases} \quad (2)$$

where α and λ are parameters.

In the case of system (2), the attractor is glued together from two centrally symmetric halves—the “half-attractors” A^+ and A^- [see Fig. 2(b)], each of which is similar to the Lorenz attractor. The difference from the Lorenz attractor is that the twin half-attractors contain three equilibria $O, O_1,$ and O_2 . These equilibria belong to the symmetry plane $z = 0$ and both to A^+ and A^- . The half-attractors lie on the opposite sides from $z = 0$ and $A^+ \cap A^- = W^u(O)$. Note that each of the halves is an invariant set, but it is not a true attractor by itself since it has no proper absorbing domain. On the other hand, there is an absorbing domain \mathcal{D} that contains the attractor $A^+ \cup A^-$.

The attractor for map (1) looks very similar. It consists of two centrally symmetric halves A^+ and A^- and contains one fixed point O and an orbit (O_1, O_2) of period two. In the numerically generated picture [see Fig. 2(a)], it appears that A^+ and A^- only touch each other along a curve—the unstable separatrix $W^u(O)$, like it happens in the case of the flow. However, because the map (1) does not have the mirror symmetry, we expect that splitting of $W^u(O)$ with $W^s(O_1)$ and $W^s(O_2)$ exists, and hence, there is no invariant surface separating A^+ and A^- , contrary to the continuous-time case.

The numerically generated trajectories in the conjoined-twins attractor of map (1) have the following property: the sequence of every second point in the orbit looks like a discretized trajectory of a system of ordinary differential equations. We explain this by the fact that this attractor has been found for parameter values close to $A = -1, B = 1, C = 1$, where this map has a fixed point with multipliers $(-1, -1, 1)$. Therefore, the map in certain coordinates is close

to the normal form for this codimension-3 bifurcation. It follows from the general theory^{47–49} that the second iteration of the normal form in this case is discretization of an axis-symmetric system of differential equations. As is shown in Ref. 50, when there are no additional symmetries, this system is close to the axially symmetric Shimizu–Morioka model, which has the Lorenz attractor.^{51–53} This fact has played an important role in the discovery of the discrete Lorenz attractor in the 3D Hénon map.⁴³ In our case, the map (1) has additionally the central symmetry; therefore, the normal form must be different and be both axially and centrally symmetric. For this case, a normal form was proposed in Ref. 50 for which the existence of a mirror-symmetric pair of well-separated Lorenz attractors was shown for some parameter values. We do not observe such attractors in map (1). Therefore, we have chosen a centrally and axially symmetric system (2) as a candidate of a normal form different from those presented in Ref. 50; the visual resemblance of the attractors in map (1) and system (2) supports this choice.

Already in the first works devoted to the Lorenz attractor, much attention was paid to the study of scenarios for its appearance in parametric families of systems; see, e.g., Ref. 20. Similar phenomenological scenarios in the case of discrete Lorenz attractors were proposed in Refs. 44 and 54, where examples of the implementation of these scenarios were given for 3D Hénon maps. Following this program, we propose the main scenario for the appearance of the conjoined Lorenz twins in one-parameter families of both centrally symmetric maps and axially and centrally symmetric flows; see Sec. II. In essence, this gives a generalization of the classical scenario²⁰ of emergence of the Lorenz attractor to the case of systems with three singularity points (three equilibria in the continuous-time case or one fixed point and one period-2 orbit in the discrete-time case). For map (1), in Sec. III, we follow this scenario numerically for fixed $B = 0.7$.

We verified numerically the pseudohyperbolicity of the conjoined Lorenz twins in both map (1) and flow (2). The procedure and results are described in Sec. IV. We stress that our method establishes reliably the chaoticity of the attractor and the robustness of the chaoticity with respect to small perturbations. Thus, we not only check the positivity of Lyapunov exponents, but we also check the continuity of certain invariant subspaces E^{ss} and E^{cu} , which, according to Turaev–Shilnikov theory,^{6,7} guarantees the robustness of the positivity of the maximal Lyapunov exponent.

II. FROM A STABLE POINT TO THE CONJOINED LORENZ TWINS.

The universal scenario we propose is very similar for 3D flows and maps. However, in the case of flow, it is simpler; therefore, we start with it.

A. Description of the scenario for one-parameter families of flows

Let us consider a one-parameter family of systems of ODEs,

$$\dot{X} = F(X, \mu), \quad (3)$$

where $X = (x, y, z)$ and μ is a parameter. Suppose that F possesses the central and axial symmetries,

$$S_c : x \rightarrow -x, \quad y \rightarrow -y, \quad z \rightarrow -z,$$

$$S_a : x \rightarrow -x, \quad y \rightarrow -y, \quad z \rightarrow z.$$

The composition of these two symmetries gives also the mirror symmetry

$$S_m : x \rightarrow x, \quad y \rightarrow y, \quad z \rightarrow -z.$$

As a result, family (3) possesses the invariant plane $z = 0$. Due to the symmetries, it is enough to describe bifurcations only for the half-space $z \geq 0$. The corresponding phase portraits are shown in Fig. 3.

We start with the simplest situation—when, initially, the attractor is the stable equilibrium $O(0, 0, 0)$. For more definiteness, we also assume that the boundary of its absorbing domain in the half-space $z \geq 0$ is formed by the stable two-dimensional manifold of a saddle equilibrium S_1 , Fig. 3(a), and that the saddle S_1 does not bifurcate for the entire range of parameter's change [note that system (2) has no equilibria S_1 and S_2 ; however, one can think that they are at infinity: indeed, they appear at large z after a small perturbation, e.g., when adding the cubic term βz^3 to the third equation of (2)].

In our scenario, we assume that with the increase of μ , the equilibrium O undergoes, at some $\mu = \mu_{PF_0}$, a supercritical pitchfork bifurcation. As a result, at $\mu > \mu_{PF_0}$, O becomes saddle and

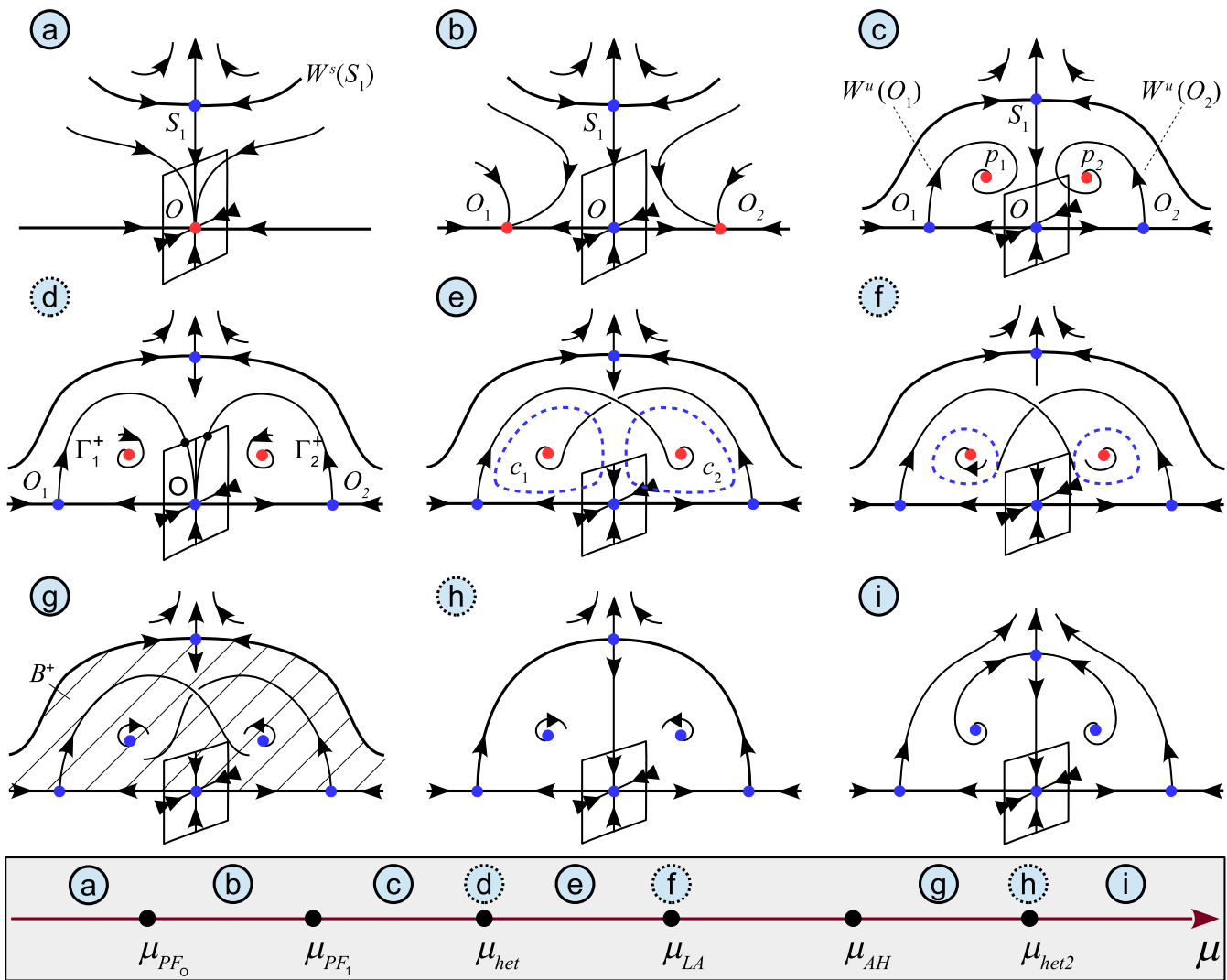


FIG. 3. Sketch of the bifurcation scenario for one-parameter families of flows (3) possessing the S_c - and S_a -symmetries: (a)–(g) from the stable point O to the half-attractor A^+ and (h)–(i) the crisis of the attractor. For maps, the bifurcation scenario is very similar: just the pair (O_1, O_2) becomes an orbit of period-2, and also, separatrices get split as in Fig. 4.

a pair of stable equilibria O_1 and O_2 is born in the plane $z = 0$, Fig. 3(b) (this bifurcation occurs inside the plane $z = 0$ due to the S_m -symmetries). Since the plane $z = 0$ is invariant, the unstable separatrices $W^u(O)$ remain in this plane and go to the equilibria O_1 and O_2 . With the further increase of μ , the equilibria O_1 and O_2 both undergo, at $\mu = \mu_{PF_1}$, a supercritical pitchfork bifurcation (due to the S_m -symmetry). Here, after the bifurcation, a pair of stable equilibria p_1 and p_2 is born in the half-space $z > 0$, Fig. 3(c). The corresponding one-dimensional unstable separatrices $W^u(O_1)$ and $W^u(O_2)$ tend to the stable equilibria p_1 and p_2 , respectively.

The next important bifurcation, at $\mu = \mu_{het}$, is the global bifurcation corresponding to that unstable separatrices of O_1 and O_2 reach the saddle O . Thus, a *heteroclinic butterfly* Γ^+ is created (in the region $z \geq 0$). It consists of two heteroclinic cycles Γ_1^+ and Γ_2^+ . Each cycle Γ_i^+ is composed from the equilibria O , O_i and their corresponding one-dimensional unstable separatrices; see Fig. 3(d). Here, we suppose that these heteroclinic cycles are unstable, i.e., the sum of *saddle values* of equilibria O and O_i and, symmetrically, O and O_2 are positive (recall that the saddle value of an equilibrium is the sum of negative and positive real parts of the nearest to the imaginary axis eigenvalues). Therefore, when the heteroclinic cycles split outward, at $\mu > \mu_{het}$, a pair of saddle periodic orbits c_1 and c_2 is born from the butterfly Γ^+ , Fig. 3(e). It is important to note that, simultaneously, a nontrivial singular hyperbolic invariant set Λ^+ containing the saddle equilibria O , O_1 , and O_2 is formed (like in the Lorenz model after the splitting of a homoclinic butterfly^{20,37,55,56}). Also, note that at $\mu > \mu_{het}$, the unstable separatrices of equilibria O_1 and O_2 rearrange: $W^u(O_1)$ goes to p_2 and $W^u(O_2)$ goes to p_1 , Fig. 3(e).

With the further increase in μ , the periodic orbits c_1 and c_2 decrease in size, and, at $\mu = \mu_{LA}$, the unstable separatrices $W^u(O_1)$ and $W^u(O_2)$ lie on the two-dimensional stable manifolds of c_1 and c_2 , Fig. 3(f). Immediately after this, the set Λ^+ becomes attracting, and we call it a *heteroclinic Lorenz-like half-attractor* A^+ . This half-attractor contains three equilibria O , O_1 , and O_2 and their unstable separatrices. At first, in the region $z \geq 0$, the half-attractor A^+ coexists with a pair of stable equilibria p_1 and p_2 . The further evolution of dynamics proceeds in one of the two following ways:

- At $\mu = \mu_{AH}^{sub}$, the periodic orbits c_1 and c_2 merge, respectively, with the stable equilibria p_1 and p_2 as a result of a subcritical Andronov–Hopf bifurcation. The same bifurcation also takes place in the Lorenz system.²⁰
- At $\mu = \mu_{AH}^{sup}$, the stable equilibria p_1 and p_2 undergo a supercritical Andronov–Hopf bifurcation, and, as a result, a pair of stable periodic orbits s_1 and s_2 is born. Then, at $\mu = \mu_{SN}$, these stable periodic orbits merge with the saddle periodic orbits c_1 and c_2 and disappear. A similar situation is observed, e.g., in the Shimizu–Morioka system.^{51,53,57}

The bifurcations at $\mu = \mu_{AH}^{sub}$ in the first case, and at $\mu = \mu_{SN}$, in the second case, are important: when $\mu > \mu_{AH}^{sub}$ or, respectively, $\mu > \mu_{SN}$, there is no longer multistability in the system. Namely, A^+ becomes the only attractive set in the half-basin B^+ [the part of the space between the surfaces $W^s(S_1)$ and $z = 0$; see Fig. 3(g)]. Accordingly, A^- is the only attractive set in the half-basin B^- .

As μ increases, the basin B^+ exists and the half-attractor A^+ remains until $\mu = \mu_{het_2}$ when the upper separatrix $W^u(O_1)$ lies on $W^s(S_1)$ and $W^u(O_2)$ does the same by the symmetry, Fig. 3(h).

Therefore, the value $\mu = \mu_{het_2}$ corresponds to the crisis of the attractor: it breaks down and orbits start to go to infinity at $\mu > \mu_{het_2}$; see Fig. 3(i).

As we noted above, the same sequence of bifurcations occurs in the half-space $z \leq 0$. Thus, at $\mu \in (\mu_{LA}, \mu_{het_2})$, a pair of half-attractors A^+ and A^- exist in system (3). These half-attractors are symmetrical to each other and contain the same equilibrium states O , O_1 and O_2 . Together, they compose the *conjoined Lorenz twins* $A = A^+ \cup A^-$ that become the only attractor in the absorbing domain $B = B^+ \cup B^-$ when $\mu > \mu_{AH}^{sub}$ or $\mu > \mu_{SN}$.

B. Description of the scenario for one-parameter families of 3D maps

In the case of three-dimensional diffeomorphisms, one can imagine a sequence of bifurcations, similar to those in the case of flow (Fig. 3), that lead to the birth and, then, to the crisis of discrete conjoined Lorenz twins. Thus, we consider a one-parameter family of maps,

$$\bar{X} = G(X, \mu), \quad (4)$$

where $X = (x, y, z)$ and μ is a parameter. Assume that G possesses the S_c -symmetry. However, we do not require the existence of the axial symmetry S_a here. This requirement is replaced by the condition that the fixed point O acquires a pair of negative multipliers; see Sec. III. Consequently, the transition between Figs. 3(a) and 3(b) happens due to a supercritical period-doubling bifurcation resulting in the birth of a stable period-2 orbit (O_1, O_2) , which is also centrally symmetric.

All the further stages of the continuous-time scenario presented in Fig. 3 are transferred almost one-to-one to the case of maps. Therefore, in order not to repeat ourselves, below, we describe only the differences between the continuous and discrete-time scenarios.

The most essential difference is in the organization of homoclinic and heteroclinic orbits, which, in the discrete-time case, exist for parameter values from some intervals, whereas for the flows, the heteroclinic connections split as parameter varies. Thus,

- The heteroclinic intersection between $W^u(O_1)$ and $W^s(O)$ [and, simultaneously, between $W^u(O_2)$ and $W^s(O)$] exists at $\mu \in (\mu_{het}^1, \mu_{het}^2)$; see Fig. 4(a) and compare it with Fig. 3(d). We suppose that the corresponding heteroclinic cycles [containing the fixed point O , the period-2 orbit (O_1, O_2) , and their heteroclinic orbits] are unstable; i.e., the product of saddle values of orbits O and (O_1, O_2) is greater than 1 (recall that in the case of maps, the saddle value of a periodic orbit is the absolute value of the product of the nearest to the unit circle stable and unstable multipliers). Then, at some $\mu > \mu_{het}^2$, a two-component saddle invariant curve (c_1, c_2) is formed out of this heteroclinic configuration: c_1 is mapped to c_2 and vice versa.
- The heteroclinic intersection between $W^u(O_1)$ and $W^s(c_2)$ [and, by the symmetry, between $W^u(O_2)$ and $W^s(c_1)$] exists also at some interval $\mu \in [\mu_{LA}^1, \mu_{LA}^2]$. The discrete heteroclinic Lorenz-like attractor appears after its splitting at $\mu > \mu_{LA}^2$.
- The heteroclinic connection between $W^u(O_1)$ and $W^s(S_1)$ [and, by the symmetry, between $W^u(O_2)$ and $W^s(S_1)$] exists at $\mu \in [\mu_{het_2}^1, \mu_{het_2}^2]$; see Fig. 4(b) and compare it with Fig. 3(h).

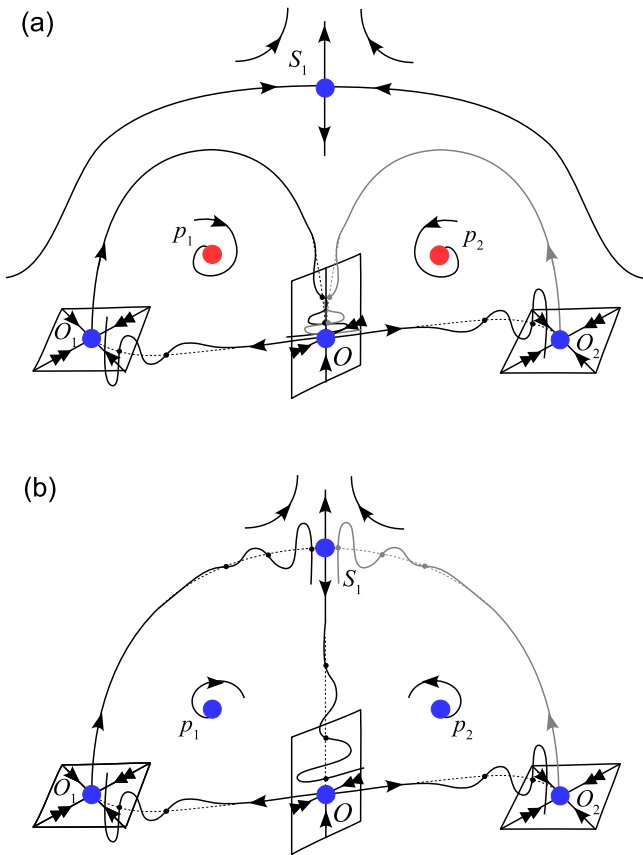


FIG. 4. Schematic pictures of heteroclinic splitting—here, only one-dimensional separatrices of points O , O_1 , O_2 , and S_1 are shown: (a) discrete analog of Fig. 3(d) and (b) discrete analog of Fig. 3(h). For map (1), the splitting is hard to detect numerically, and the separatrices look-alike is shown by the dotted lines.

The crisis of the heteroclinic attractor occurs just after the first tangency at $\mu > \mu_{het_2}^1$.

- It is important to note that we assume that the heteroclinic intersection between $W^u(O)$ and $W^s(O_i)$ exists for all μ . In general, the manifolds $W^u(O)$ and $W^s(O_i)$ are split; see Fig. 4. However, the splitting of invariant manifolds $W^u(O)$ and $W^s(O_i)$ can be extremely small; e.g., it is invisible in our numerical experiments with map (1). Due to this splitting, orbits from one part of the conjoined attractors can, in principle, pass to the other part.

III. CONJOINED LORENZ TWINS IN THE 3D MAP (1)

In this section, we give an example of the implementation of the above scenario for map (1) at $B = 0.7$.

For this purpose, we construct the Lyapunov diagram in the (A, C) -parameter plane; see Fig. 5. We also show main bifurcation curves in this figure. The curves were computed using the MatContM software package.^{58–60} Dashed lines (*het* and *het*₂) are actually not curves but thin strips; they correspond to the existence of

heteroclinic intersections between the invariant manifolds of certain saddle points. In the diagram, the yellow- and red-colored regions correspond to parameter values where a numerically found attractor is chaotic (i.e., numerically estimated maximal Lyapunov exponent Λ_1 is positive). Moreover, for the red-colored region, the attractor is pseudohyperbolic (see Sec. IV); this guarantees that the chaoticity in the red-colored region is robust, whereas in the yellow-colored region, stability windows (colored green or blue) are possible. The green- and blue-colored regions correspond to parameter values where the attractor is simple—a stable periodic orbit or, respectively, a stable closed invariant curve. At the parameter values from the white-colored regions, orbits from a neighborhood of the origin escape to infinity; see the color coding in the right palette in Fig. 5 (the Lyapunov exponents $\Lambda_1 \geq \Lambda_2 > \Lambda_3$ were calculated by iterations of initial points close to $O(0, 0, 0)$ using the standard method of Ref. 61).

In the region T_0 , map (1) has the fixed point $O(0, 0, 0)$ as the only attractor. The absorbing domain for this point (and for all attractors, which will develop from it) is bounded by the two-dimensional stable manifolds of saddle fixed points $S_1(p, p, p)$ and $S_2(-p, -p, -p)$, where $p = \sqrt{2(1 - A - B - C)}$; cf. Fig. 3(a).

The stability region T_0 for the fixed point O is bounded by three bifurcation curves. The right boundary of T_0 is the pitchfork bifurcation curve $PF_0: C = 1 - A - B$ on which the saddles S_1 and S_2 merge with the point O . Thus, above the curve PF_0 , map (1) has only one fixed point $O(0, 0, 0)$ and it is saddle. The left boundary of T_0 is formed by a supercritical period-doubling bifurcation curve $PD_0: C = 1 + A + B$. Above this curve, the point O becomes saddle, and a stable period-2 orbit (O_1, O_2) is born from it; see Figs. 6(a) and 3(b). We recall that map (1) is centrally symmetric, and the orbit (O_1, O_2) is also centrally symmetric: $O_2 = S_c(O_1)$. The bottom boundary of the stability region T_0 is formed by the supercritical Andronov–Hopf bifurcation curve $C = B^2 - AB - 1$, $-2 < A - B < 2$ (not shown in Fig. 5).

The stable period-2 orbit (O_1, O_2) undergoes a supercritical pitchfork bifurcation when crossing the curve PF_1 . As a result, above this curve, the orbit (O_1, O_2) becomes saddle, and an S_c -symmetric pair of stable period-2 orbits, (p_1, p_2) and (p_3, p_4) appears in its neighborhood. The orbit (p_1, p_2) resides above the line $[O_1, O, O_2]$ and the orbit (p_3, p_4) below, as shown in Figs. 6(b) and 3(c). Note that just after these bifurcations, the unstable separatrices $W^u(O_1)$ and $W^u(O_2)$, which are above the line $[O_1, O, O_2]$, go to the points p_1 and p_2 , respectively. Symmetrically, the separatrices below the line $[O_1, O, O_2]$ go to p_3 and p_4 . Furthermore, we discuss the dynamics only in the half-space above the line $[O_1, O, O_2]$.

The unstable separatrices $W^u(O_1)$ and $W^u(O_2)$ rearrange when the parameters cross the very thin heteroclinic zone *het*, in which $W^u(O_1)$ and $W^u(O_2)$ intersect with $W^s(O)$ and thus, the heteroclinic butterfly (a pair of heteroclinic cycles Γ_1^+ and Γ_2^+) exists; see Figs. 6(c), 3(d), and 4(a). The heteroclinic butterfly is unstable. Therefore, when it splits outward upon crossing the zone *het* from right to left, a two-component saddle invariant curve (c_1, c_2) is formed, as shown in Figs. 6(d) and 3(e). Now, the unstable separatrix $W^u(O_1)$ tends to the point p_2 , while $W^u(O_2)$ tends to p_1 .

The conjoined Lorenz twins attractor is born upon crossing the thin region *LA* separating the red-colored region from the green-colored region in Fig. 5 (see the left inset). For parameter values

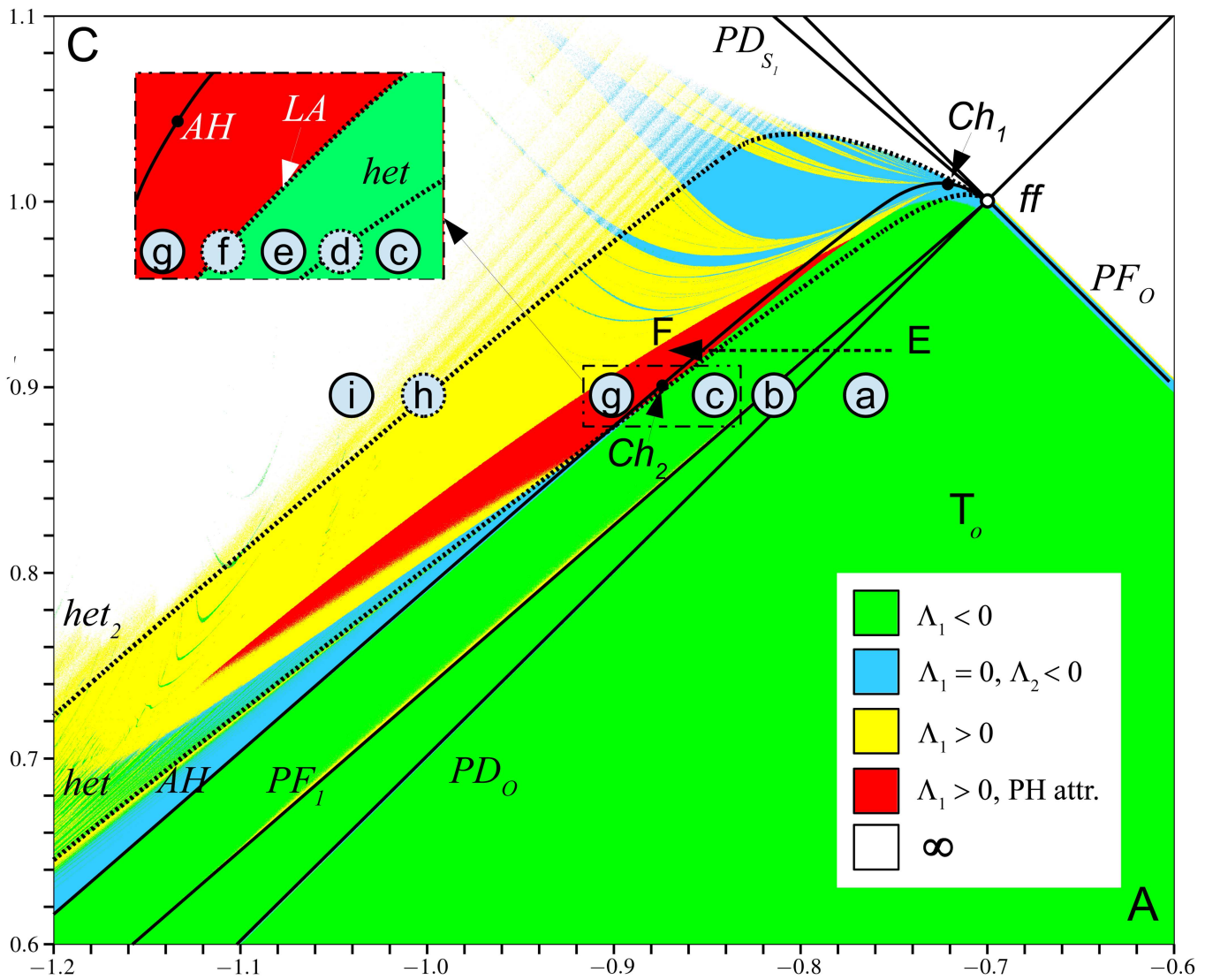


FIG. 5. Lyapunov diagram and some bifurcation curves for map (1) on the (A, C) -parameter plane when $B = 0.7$. Different colors correspond to different types of attractors (see the palette in the bottom-right corner), which is obtained by iterations of some initial point taken near the origin; red color corresponds to the region with the pseudo-hyperbolic attractor (here, it is the conjoined Lorenz twins); see more details in Sec. IV. Between the curves PF_0 and PD_0 , the fixed point $O(0, 0, 0)$ is stable [Fig. 3(a)], PF_0 —subcritical pitchfork bifurcation for O ; PD_0 —supercritical period-doubling bifurcation of point O , above this curve, the stable period-2 orbit (O_1, O_2) is born near O , like in Fig. 3(b); PF_1 —supercritical pitchfork bifurcation of the period-2 orbit (O_1, O_2) ; above this curve, a pair of stable period-2 orbits (p_1, p_2) and (p_3, p_4) is born, like in Fig. 3(c); thin wedges het , LA , and het_2 correspond to heteroclinic bifurcations, like shown in Figs. 3(d), 3(f), and 3(h), respectively; AH —Andronov–Hopf bifurcations with (p_1, p_2) and (p_3, p_4) , this bifurcation is subcritical between the Chenciner points Ch_1 and Ch_2 . The curves PD_0 , PF_1 , AH , PD_{S_1} , PF_0 and extremely thin wedges het and het_2 start from the fold-flip point ff ($B = 0.7, A = -0.7, C = 1$). The pathway EF : $A = -0.92, C \in [-0.74, -0.86]$ is that along which we study the scenario of the discrete conjoined Lorenz twins appearance; see Fig. 6.

from LA , the separatrices $W^u(O_1)$ and $W^u(O_2)$ intersect with the two-dimensional stable manifold of the saddle period-2 curves c_2 and c_1 , respectively (numerically, it looks like that the unstable separatrices lie completely in the stable manifolds of c_1 and c_2), Figs. 6(e) and 3(f).

At the beginning, the conjoined-twins attractor coexists with the stable period-2 orbits (p_1, p_2) and (p_3, p_4) . The segment of the curve AH between the points Ch_1 and Ch_2 corresponds to a subcritical Andronov–Hopf bifurcation—when crossing this curve, the saddle invariant curves (c_1, c_2) and (c_3, c_4) merge, respectively, with

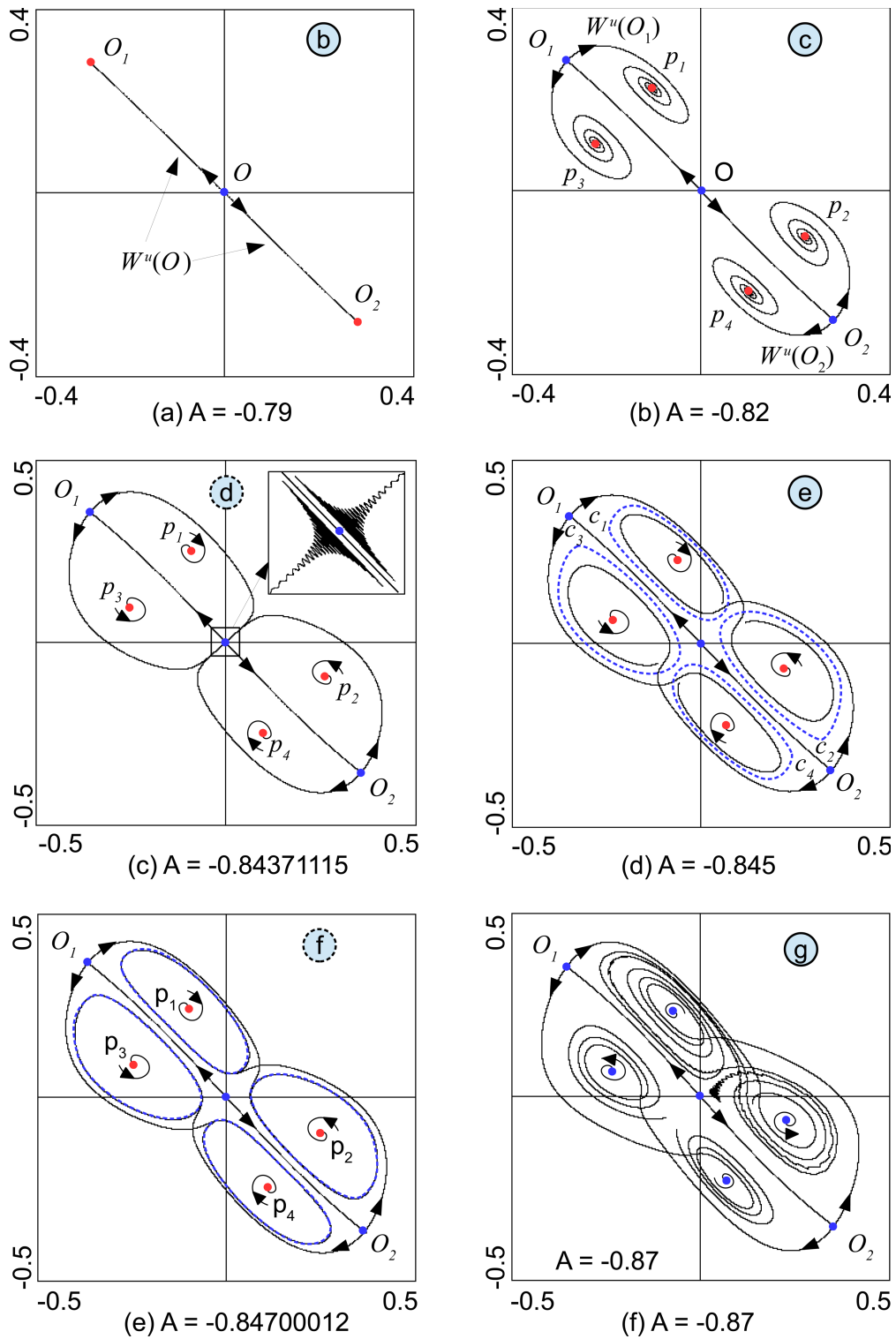


FIG. 6. Illustration for the bifurcation scenario leading to the emergence of the conjoined Lorenz twins in map (1) along the pathway EF shown in Fig. 5.

the stable periodic orbits (p_1, p_2) and (p_3, p_4) , which become saddle after that (points Ch_1 and Ch_2 correspond to the Chenciner bifurcation⁶²—a degenerate Andronov–Hopf bifurcation for maps, and divide the curve AH into segments—corresponding to the supercritical and subcritical bifurcations). Since the Andronov–Hopf bifurcation along the pathway EF (see Fig. 5) is subcritical, the conjoined Lorenz twins immediately become the only attractor of map (1), Figs. 6(f) and 3(g).

The attractor undergoes crisis when parameter values cross the thin strip het_2 where the unstable separatrices $W^u(O_1)$ and $W^u(O_2)$ intersect with the two-dimensional stable manifolds of the saddle fixed point S_1 and S_2 . The corresponding configuration of invariant manifolds for S_1 is shown schematically in Fig. 4(b) (symmetrically for S_2). Upon crossing het_2 , orbits start to run to infinity, Fig. 3(i).

In Fig. 6, the behavior of the one-dimensional unstable manifolds $W^u(O)$ and $W^u(O_i)$ is shown for map (1) as the parameter A changes along the pathway EF : $B = 0.7$, $C = 0.95$, $A \in [-0.7, -0.85]$. Figures 6(a), 6(b), and 6(d) correspond to the schematic phase portraits presented in Figs. 3(b), 3(c), and 3(e), respectively. In Fig. 6(c), the creation of four heteroclinic cycles is shown. Here, one can see that the invariant manifolds $W^u(O_i)$ and $W^s(O)$ are indeed splitted as discussed in Sec. II B [cf. Fig. 4(a)]. These heteroclinic cycles are unstable since the product of saddle values $\sigma(O)$ and $\sigma(O_1, O_2)$ is greater than 1 ($\sigma(O) = 1.058$ and $\sigma(O_1, O_2) = 1.165$). Therefore, a pair of two-component saddle invariant curves (c_1, c_2) and (c_3, c_4) emerges soon after the splitting of these cycles; see Fig. 6(c) [an analog of the schematic phase portrait shown in Fig. 4(a)]. The heteroclinic connections between $W^u(O_i)$ and these invariant curves are shown in Fig. 6(e) [an analog of Fig. 3(f)]. The discrete conjoined Lorenz twins are born immediately after this connection disappears; see Fig. 6(f) [an analog of Fig. 3(g)].

It is worth noting that the bifurcation curves PD_O, PF_1, AH, PD_{S_1} , and PF_O , as well as the thin strips het and het_2 , corresponding to heteroclinic bifurcations, all go out of the fold-flip point ff , where the fixed point O has multipliers $(-1, 1, -B)$. Because of the central symmetry, this bifurcation proceeds differently from the general fold-flip case studied in Ref. 63. Instead, the local bifurcation diagram is similar to that for equilibria with two pairs of pure-imaginary eigenvalues.^{64,65} The region with a chaotic attractor does not join to the point ff but tends to it as $B \rightarrow 1$. This observation allows us to propose conjecture on the birth of the conjoined Lorenz twins from bifurcations of a fixed point with the triplet of multipliers $(-1, -1, 1)$ in maps with the central symmetry.

IV. ON PSEUDOHYPERBOLIC PROPERTIES OF THE ATTRACTORS

In this section, for the attractors under consideration, we study the question of robustness, i.e., pseudohyperbolicity, of chaos with respect to small perturbations, including bounded noise.

The pseudohyperbolicity of a strange attractor guarantees the existence of a positive maximal Lyapunov exponent for all its orbits. The pseudohyperbolicity is much weaker than the hyperbolicity, and therefore, pseudohyperbolic attractors are much more common in applications than hyperbolic ones. In this regard, the verification of

the pseudohyperbolicity of attractors takes the first priority in the general problem of studying their dynamics.

In our case, both map (1) and flow (2) are three-dimensional, and chaotic attractors observed in these systems have one positive, one zero, or, in the case of maps, near-zero, and one strongly negative Lyapunov exponents. Therefore, we can assume that the differential of the system [map (1) or flow (2)] allows for the splitting of the tangent space into invariant subspaces E^{ss} (one-dimensional) and E^{cu} (two-dimensional). To verify the pseudohyperbolicity, we need to check that⁶⁷

- such splitting exists at every point of the attractor and depends continuously on the point;
- E^{ss} corresponds to strongly contracting directions (stronger than any possible contraction in E^{cu}); and
- the differential of a system expands two-dimensional areas in E^{cu} .

Numerical methods for the verification of these conditions were developed in Refs. 1 and 66; see also Ref. 67. For checking conditions (B) and (C), one just should calculate the spectrum of Lyapunov exponents and check that the following conditions hold:

- $\Lambda_2 > \Lambda_3$, which implies condition (B) and
- $\Lambda_1 + \Lambda_2 > 0$, which implies condition (C).

Both these conditions are fulfilled for the attractors presented in Fig. 2 since $\Lambda_1 = 0.014\ 68 \pm 4 \times 10^{-5}$, $\Lambda_2 = 0.000\ 13 \pm 3 \times 10^{-5}$, $\Lambda_3 = -0.371\ 49 \pm 4 \times 10^{-5}$ —for the discrete half-attractors shown in Fig. 2(a); and $\Lambda_1 = 0.061\ 75 \pm 1.5 \times 10^{-4}$, $\Lambda_2 = \pm 1.4 \times 10^{-5}$, $\Lambda_3 = -1.311\ 75 \pm 1.5 \times 10^{-4}$ —for the flow half-attractors shown in Fig. 2(b).

We check that condition (A) is a much more delicate and difficult problem. It is based on the calculation of Lyapunov co-variant vectors^{68,69} and construction of the so-called E^{ss} - and E^{cu} -continuity diagrams, as was proposed in Ref. 1, and computing the angles between E^{ss} and E^{cu} , as was done in Ref. 67. Since in our case, the subspace E^{cu} has codimension 1, the continuous dependence of E^{cu} on the phase space point is equivalent to the continuity of the field of normals N^{cu} to E^{cu} .

The E^{ss} -continuity diagram is a graph showing how angles $\varphi(v_i, v_j)$ between Lyapunov co-variant vectors $v_i \in E^{ss}(x_i)$ and $v_j \in E^{ss}(x_j)$ depend on the distance $\rho(x_i, x_j)$ between x_i and x_j for any pair of points x_i and x_j in the attractor; see Ref. 1. Similarly, the N^{cu} -continuity diagram is built in the (ρ, φ) -plane for vectors from N^{cu} . If $\varphi(v_i, v_j)$ tends to zero when $\rho(x_i, x_j) \rightarrow 0$, one can conclude that the subspaces E^{ss} and N^{cu} depend continuously on the point of the attractor. If, at $\rho(x_i, x_j) \rightarrow 0$, the angles $\varphi(v_i, v_j)$ take arbitrary values, then the attractor is definitely non-pseudohyperbolic.

The calculation of angles between the subspaces E^{ss} and E^{cu} at each numerically generated point of the attractor is also useful due to the fact that the E^{ss} - and E^{cu} -continuity conditions imply the absence of tangencies between the corresponding subspaces.⁶⁶

Numerical results obtained with the help of both methods for the half-attractors A^+ shown in Fig. 2 are presented in Fig. 7. In the top row, we present the results of checking condition (A) for the discrete half-attractor A^+ [colored in blue in Fig. 2(a)] of map (1) for $(A, B, C) = (-0.9, 0.7, 0.9)$; in the bottom—for the flow

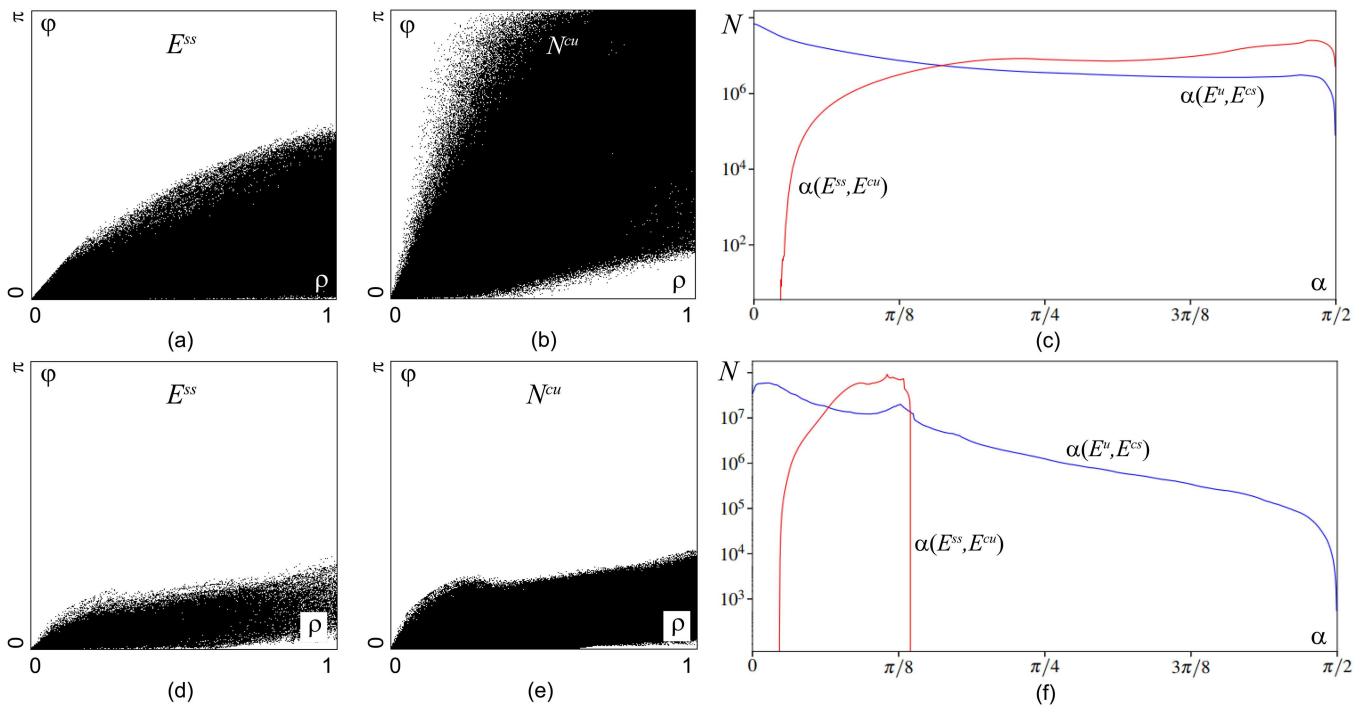


FIG. 7. Results of numerical verification of the half-attractors A^+ shown in Fig. 2 on pseudohyperbolicity: top row—for the discrete attractor from Fig. 2(a) and bottom row—for the flow attractor from Fig. 2(b). The graphs in first and second columns show that the subspaces E^{ss} and N^{cu} , respectively, depend continuously on points of the attractor since $\varphi(\rho) \rightarrow 0$ when $\rho \rightarrow 0$. Red- and blue-colored curves in the third column depict the distribution of angles between E^{ss} and E^{cu} and E^u and E^{cs} , respectively. Together, these results show that the attractors are pseudohyperbolic but not hyperbolic (the blue curves of graphs from the third column confirm the later).

half-attractor A^+ [colored in blue in Fig. 2(b)] in system (2) for $(\alpha, \lambda) = (0.4, -0.15)$.

The E^{ss} - and N^{cu} -continuity diagrams shown in Figs. 7(a) and 7(b) confirm that the subspaces E^{ss} and E^{cu} depend continuously on the point of the discrete half-attractor A^+ . The red-colored curve in Fig. 7(c) corresponds to the distribution of angles between E^{ss} and E^{cu} . The angles were estimated along 1600 different orbits on the half-attractor A^+ , and the length of each orbit is 10^7 . The red-colored curve does not touch the line $\alpha = 0$ of zero angles, which confirms the absence of tangencies between the subspaces E^{ss} and E^{cu} . These results allow us to conclude that the half-attractor A^+ presented in Fig. 2(a) is pseudohyperbolic. The half-attractor A^- is pseudohyperbolic by the symmetry.

The blue-colored line in Fig. 7(c) shows the distribution of angles between other two subspaces: E^u , which is composed from covariant vectors corresponding to the maximal Lyapunov exponent Λ_1 , and E^{cs} , which corresponds to other two Lyapunov exponents Λ_2 and Λ_3 . Zero angles in this graph confirm that these subspaces are non-transversal, and therefore, the attractor cannot be hyperbolic. Moreover, this suggests that the attractor is wild due to the possibility of the existence of homoclinic and heteroclinic tangencies.

Independently, the wildness is confirmed by the computation of the unstable separatrices $W^u(O_i)$; see the black-colored curves in Fig. 8(a). In this figure, one can see that the unstable separatrices of

the points O_1 and O_2 strongly oscillate, and thus, there is no possibility to avoid homoclinic tangencies with stable manifolds of periodic orbits belonging to the attractor.

After the establishment of pseudohyperbolicity of the half-attractor A^+ (and, by symmetry, A^-), the question arises whether

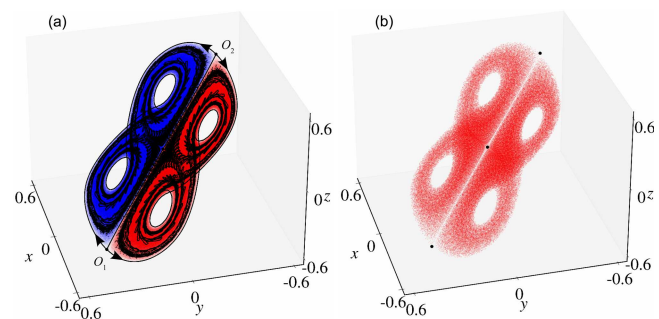


FIG. 8. (a) Unstable separatrices $W^u(O_i)$ for the attractor shown in Fig. 2(a). (b) Merger of two halves of the conjoined Lorenz twins presented in Fig. 2(a) into a single *double Lorenz attractor* after the addition of noise with the amplitude 0.001 to the right side for \bar{z} in map (1). As usual for homoclinic attractors, the neighborhood of its fixed point is the least visited part of the attractor by orbits—therefore, one can see a white thin strip between the point O_1 and O_2 .

the entire attractor $A^+ \cap A^-$ is pseudohyperbolic? In other words, do the subspaces E^{ss} and E^{cu} change continuously at the transition from A^+ to A^- ? In order to answer this question, we perform a series of experiments with the attractor of map (1) under the action of bounded noise with a small amplitude (the noise makes the jumps between A^+ and A^- visible and allows the numerically generated trajectory to come closer to the boundary between A^+ and A^-). We add the noise with the amplitude 0.001 to the right-hand side of the equation for \bar{z} in (1). The resulting attractor is shown in Fig. 8(b). The E^{ss} - and E^{cu} -continuity diagrams, as well as the graph of the distribution of angles between these subspaces, do not principally differ from the graph shown in Figs. 7(a)–7(c). This confirms the continuity of E^{ss} and E^{cu} and, thus, the pseudohyperbolicity of the conjoined Lorenz twins in Fig. 8(b).

The same series of experiments was conducted for the flow half-attractor A^+ plotted in Fig. 2(b) in blue; see Figs. 7(d)–7(f). These experiments show that this half-attractor is also pseudohyperbolic but not hyperbolic. However, it cannot be wild due to the existence of the strongly stable foliations, which prevents from homoclinic tangencies in 3D flows.

Not all chaotic attractors in map (1) and in system (2) are pseudohyperbolic. In Fig. 9, we present an example of non-pseudohyperbolic discrete conjoined twins. It looks very similar to the attractor shown in Fig. 2(a). However, the E^{ss} - and E^{cu} -continuity conditions are violated here, as is given by Figs. 9(c) and 9(d). Zero angles between the subspaces E^{ss} and E^{cu} [Fig. 9(b)] also confirm the violation of the pseudohyperbolicity. According to the “P or Q” conjecture from Ref. 1, one can expect here that small perturbations can create stable periodic orbits making the chaos transient (i.e., the numerically observed chaotic attractor is, in fact, a quasiattractor in the Afraimovich–Shilnikov sense⁷⁰).

In order to distinguish between the regions with pseudohyperbolic and non-pseudohyperbolic chaos, we, for fixed $B = 0.7$, computed the minimal angle between the subspaces E^{ss} and E^{cu} for chaotic attractors of map (1) for a fine grid in the (A, C) -parameter plane. If the minimal angle estimated by 10^7 iterations of an orbit taken on the attractor was greater than a threshold value 0.0001, we consider the pseudohyperbolicity condition (A) to be fulfilled. Also, in this experiment, we check whether all multipliers of the period-2 saddle point (O_1, O_2) are real (in 3D maps, chaotic attractors containing saddle-focus periodic orbits cannot be pseudohyperbolic). The verification of this additional condition has allowed us to exclude some chaotic attractors for which the conditions (A)–(C) were fulfilled numerically from the candidates for pseudohyperbolicity. Parameter values corresponding to chaotic attractors that have passed the verification of all the described conditions populate the red-colored region in Fig. 5. The complementary yellow-colored region corresponds to non-pseudohyperbolic attractors. Thus, chaos in this region is not robust, which is confirmed by the stability windows (colored in green and blue) inside this region.

Remark 1: *When checking the pseudohyperbolicity, we perform standard double-precision computations. Thus, we can claim only “numerical evidence” for the results, in contrast to the rigorous numerics (see, e.g., Refs. 29 and 71–75), which could provide computer-assisted proofs. However, the latter are too time- and effort-consuming. On the other hand, our approach can be viewed as an exploratory one, and if there is a need, the results obtained can be*

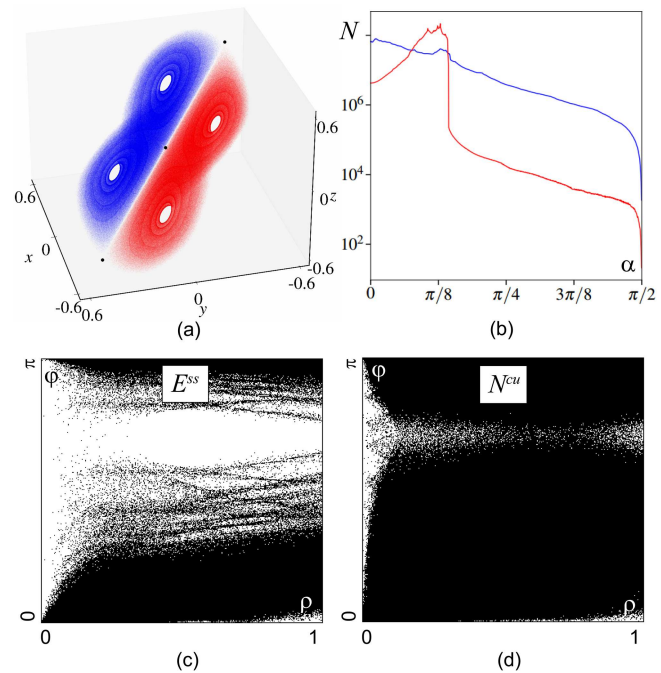


FIG. 9. Results of numerical experiments with the half-attractor A^+ existing at $B = 0.7, A = -0.92, C = 0.9$ in map (1) (this point belongs to the yellow region of the Lyapunov diagram shown in Fig. 5): (a) phase portrait of the conjoined Lorenz twins; (b) distribution of angles between E^{ss} and E^{cu} (red curve) and E^s and E^{cs} (blue curve); and (c) and (d) the E^{ss} - and N^{cu} -continuity diagrams. These results show that the conjoined attractor is definitely non-pseudohyperbolic despite it looks like the pseudohyperbolic attractor shown in Fig. 2(a).

taken as a starting point for rigorous numerics. It would be very interesting to provide a computer-assisted proof for the pseudohyperbolicity of the conjoined Lorenz twins both in map (1) and flow (2).

V. DISCUSSION

We have found new types of pseudohyperbolic attractors; see Fig. 2. Such attractors can appear in 3D maps possessing the central symmetry and in 3D flows with the central and mirror symmetries. We have demonstrated this on the examples of 3D map (1), Fig. 2(a), and 3D flow (2), Fig. 2(b).

The existence of the global symmetries is a specific and important feature of the conjoined Lorenz-like attractors both in the case of maps and flows. Note that under perturbations destroying this symmetry, the chaoticity is preserved because of the pseudohyperbolicity, but the geometry can change drastically.

The breaking down of the central symmetry can lead to a collapse of the attractor. Namely, when the separatrices of the saddle O do not intersect with the two-dimensional stable manifolds of O_1 and O_2 , the latter become separated from the attractor. In this case, if both unstable separatrices of O split up or down, then only one of the twins (A^+ or A^-) remains attracting and starts to look like the standard Lorenz attractor with one singularity. What happens when the separatrices split in different directions is beyond the scope of this paper, and we plan to return to this later.

In the case of discrete attractors, the violation of symmetry can lead to an opposite effect: the transverse intersections between $W^u(O)$ and $W^s(O_{1,2})$ and, hence, the overlap between the two half-attractors can become more visible. The resulting attractor would provide an example of the discrete double Lorenz-like attractor, as proposed in Ref. 3.

We have given a numerical evidence for the wildness of the discrete conjoined Lorenz twins. However, the existence of homoclinic intersections and tangencies of invariant manifolds of the points O , O_1 , and O_2 remains unproven. Here, it is necessary first of all to study how the unstable separatrices of the point O are split, and this is a very delicate problem that will be considered in future works.

Note also that 3D cubic Hénon-like maps possessing the central symmetry were considered in the paper¹⁶ in which the problem was outlined for constructing examples of discrete homoclinic attractors containing a saddle fixed point with a positive unstable multiplier. Here, the symmetry is needed such that both unstable one-dimensional separatrices have the same behavior and simultaneously belong or not belong to the attractor together with the saddle. In the light of the results obtained in the present paper, it seems very interesting to continue the research begun in Ref. 46 in order to develop the theory of homoclinic pseudohyperbolic attractors and to find new types of conjoined Lorenz twins. In particular, if family (4) would possess both the symmetries S_c and S_a , then the supercritical pitchfork bifurcation of the point O leading to the appearance of a pair of stable fixed points O_1 and O_2 is also possible.

Another interesting problem is related to the study of bifurcations of the birth of strange attractors in flow normal forms for bifurcations of fixed points with the multipliers $(1, 1, 1)$ and $(-1, -1, 1)$ in maps with additional symmetries. Similar problems were considered early as in Ref. 50, and we plan to generalize these results to the case of systems with the conjoined Lorenz twins.

ACKNOWLEDGMENTS

The authors thank P. Kuptsov, A. Shilnikov, and D. Turaev for fruitful discussions and useful remarks. Analytical results in Secs. I and II and the results of pseudohyperbolicity verification by the method of angles were supported by the RSF grant (No. 19-11-00280). The results of bifurcation analysis presented in Sec. III were supported by the RSF grant (No. 19-71-10048). The numerical results of pseudohyperbolicity verification by the E^{ss} - and E^{cu} -continuity method presented in Sec. IV were supported by the Laboratory of Dynamical Systems and Applications NRU HSE, of the Ministry of Science and Higher Education of the RF grant (Agreement No. 075-15-2019-1931). The authors also thank the Theoretical Physics and Mathematics Advancement Foundation “BASIS” (Grant No. 20-7-1-36-5) for the support of scientific research studies.

AUTHOR DECLARATIONS

Conflict of Interest

The authors have no conflicts to disclose.

Author Contributions

Sergey Gonchenko: Conceptualization (lead); Funding acquisition (lead); Methodology (equal); Supervision (lead); Writing – original

draft (equal). **Efrosiniia Karatetskaia:** Data curation (equal); Formal analysis (equal); Investigation (equal); Project administration (equal); Software (equal); Visualization (equal). **Alexey Kazakov:** Conceptualization (equal); Data curation (equal); Investigation (equal); Methodology (equal); Project administration (equal); Software (equal); Supervision (equal); Visualization (equal); Writing – original draft (equal). **Vyacheslav Kruglov:** Conceptualization (supporting); Data curation (lead); Formal analysis (equal); Investigation (lead); Methodology (equal); Software (lead); Validation (lead); Visualization (equal); Writing – original draft (supporting).

DATA AVAILABILITY

The data supporting numerical experiments presented in this paper are available from the corresponding author upon reasonable request.

REFERENCES

- 1 S. Gonchenko, A. Kazakov, and D. Turaev, “Wild pseudohyperbolic attractor in a four-dimensional Lorenz system,” *Nonlinearity* **34**, 2018–2047 (2021).
- 2 A. S. Gonchenko, S. V. Gonchenko, A. O. Kazakov, and A. Kozlov, “Elements of contemporary theory of dynamical chaos: A tutorial. Part I. Pseudohyperbolic attractors,” *Int. J. Bifurcat. Chaos* **28**, 1830036 (2018).
- 3 S. Gonchenko, A. Gonchenko, A. Kazakov, and E. Samylna, “On discrete Lorenz-like attractors,” *Chaos* **31**, 023117 (2021).
- 4 A. S. Gonchenko, S. V. Gonchenko, and A. O. Kazakov, “Richness of chaotic dynamics in nonholonomic models of a Celtic stone,” *Regul. Chaotic Dyn.* **18**, 521–538 (2013).
- 5 A. V. Borisov, A. O. Kazakov, and I. R. Sataev, “The reversal and chaotic attractor in the nonholonomic model of Chaplygin’s top,” *Regul. Chaotic Dyn.* **19**, 718–733 (2014).
- 6 D. Turaev and L. P. Shilnikov, “An example of a wild strange attractor,” *Sb. Math.* **189**, 291 (1998).
- 7 D. Turaev and L. P. Shilnikov, “Pseudohyperbolicity and the problem on periodic perturbations of Lorenz-type attractors,” *Dokl. Math.* **77**, 17–21 (2008).
- 8 S. Smale, “Differentiable dynamical systems,” *Bull. Am. Math. Soc.* **73**, 747–817 (1967).
- 9 R. F. Williams, “One-dimensional non-wandering sets,” *Topology* **6**, 473–487 (1967).
- 10 R. F. Williams, “Expanding attractors,” *Publ. Math. IHÉS* **43**, 169–203 (1974).
- 11 R. V. Plykin, “Sources and sinks of A-diffeomorphisms of surfaces,” *Math. USSR-Sb.* **23**, 233 (1974).
- 12 D. Anosov, G. Gould, S. Aranson, V. Grines, R. Plykin, A. Safonov, E. Sataev, S. Shlyachkov, V. Solodov, A. Starkov, and A. M. Stepin, *Dynamical Systems IX: Dynamical Systems with Hyperbolic Behaviour* (Springer, 1995), Vol. 66.
- 13 S. P. Kuznetsov, “Example of a physical system with a hyperbolic attractor of the Smale-Williams type,” *Phys. Rev. Lett.* **95**, 144101 (2005).
- 14 S. Kuznetsov and E. Seleznev, “A strange attractor of the Smale-Williams type in the chaotic dynamics of a physical system,” *J. Exp. Theor. Phys.* **102**, 355–364 (2006).
- 15 S. P. Kuznetsov and A. Pikovsky, “Autonomous coupled oscillators with hyperbolic strange attractors,” *Phys. D: Nonlinear Phenom.* **232**, 87–102 (2007).
- 16 S. P. Kuznetsov, *Hyperbolic Chaos* (Springer, 2012).
- 17 J. Marsden, “Lecture I attempts to relate the Navier-Stokes equations to turbulence,” in *Turbulence Seminar* (Springer, 1977), pp. 1–22.
- 18 R. F. Williams, “The structure of Lorenz attractors,” *Publ. Math. IHÉS* **50**, 73–99 (1979).
- 19 J. Guckenheimer and R. F. Williams, “Structural stability of Lorenz attractors,” *Publ. Math. Inst. Haut. Études Sci.* **50**, 59–72 (1979).
- 20 L. P. Shilnikov, “Bifurcation theory and the Lorenz model,” in Appendix to Russian edition of *The Hopf Bifurcation and Its Applications*, edited by J. Marsden and M. McCracken (Springer Science & Business Media, 1980), pp. 317–335.

- ²¹L. Shilnikov, “The bifurcation theory and quasi-hyperbolic attractors,” *Usp. Mat. Nauk* **36**, 240–241 (1981).
- ²²J. G. Sinai and E. B. Vul, “Hyperbolicity conditions for the Lorenz model,” *Phys. D: Nonlinear Phenom.* **2**, 3–7 (1981).
- ²³L. Bunimovich, “Statistical properties of Lorenz attractors,” in *Nonlinear Dynamics and Turbulence* (Pitman, 1983), pp. 71–92.
- ²⁴C. Robinson, “Homoclinic bifurcation to a transitive attractor of Lorenz type,” *Nonlinearity* **2**, 495 (1989).
- ²⁵M. R. Rychlik, “Lorenz attractors through Shilnikov-type bifurcation. Part I,” *Ergod. Theory Dyn. Syst.* **10**, 793–821 (1990).
- ²⁶C. Robinson, “Homoclinic bifurcation to a transitive attractor of Lorenz type, II,” *SIAM J. Math. Anal.* **23**, 1255–1268 (1992).
- ²⁷C. A. Morales, M. J. Pacifico, and E. R. Pujals, “On C1 robust singular transitive sets for three-dimensional flows,” *C. R. Acad. Sci. Ser. I-Math.* **326**, 81–86 (1998).
- ²⁸E. A. Sataev, “Some properties of singular hyperbolic attractors,” *Sb.: Math.* **200**, 35 (2009).
- ²⁹W. Tucker, “The Lorenz attractor exists,” *C. R. Acad. Sci. Ser. I-Math.* **328**, 1197–1202 (1999).
- ³⁰V. N. Belykh, N. V. Barabash, and I. V. Belykh, “A Lorenz-type attractor in a piecewise-smooth system: Rigorous results,” *Chaos* **29**, 103108 (2019).
- ³¹D. Li and D. Turaev, “Persistent heterodimensional cycles in periodic perturbations of Lorenz-like attractors,” *Nonlinearity* **33**, 971 (2020).
- ³²K. Pusuluri, H. G. E. Meijer, and A. Shilnikov, “Homoclinic puzzles and chaos in a nonlinear laser model,” *Commun. Nonlinear Sci. Numer. Simul.* **93**, 105503 (2021).
- ³³M. Malkin and K. Safonov, “Entropy charts and bifurcations for Lorenz maps with infinite derivatives,” *Chaos* **31**, 043107 (2021).
- ³⁴A. Kazakov, “On bifurcations of Lorenz attractors in the Lyubimov–Zaks model,” *Chaos* **31**, 093118 (2021).
- ³⁵V. N. Belykh, N. V. Barabash, and I. V. Belykh, “Sliding homoclinic bifurcations in a Lorenz-type system: Analytic proofs,” *Chaos* **31**, 043117 (2021).
- ³⁶D. Barros, C. Bonatti, and M. J. Pacifico, “Up, down, two-sided Lorenz attractor, collisions, merging and switching,” *arXiv:2101.07391* (2021).
- ³⁷V. S. Afraimovich, V. Bykov, and L. P. Shilnikov, “On the origin and structure of the Lorenz attractor,” *Akad. Nauk SSSR Dokl.* **234**, 336–339 (1977).
- ³⁸S. E. Newhouse, “The abundance of wild hyperbolic sets and non-smooth stable sets for diffeomorphisms,” *Publ. Math. IHÉS* **50**, 101–151 (1979).
- ³⁹S. Gonchenko, L. Shilnikov, and D. Turaev, “On models with non-rough Poincaré homoclinic curves,” *Phys. D: Nonlinear Phenom.* **62**, 1–14 (1993).
- ⁴⁰S. V. Gonchenko, D. V. Turaev, and L. P. Shilnikov, “Models with a structurally unstable homoclinic Poincaré curve,” *Dokl. Akad. Nauk* **320**, 269–272 (1991).
- ⁴¹S. Gonchenko, D. Turaev, and L. Shilnikov, “Homoclinic tangencies of arbitrarily high orders in conservative and dissipative two-dimensional maps,” *Nonlinearity* **20**, 241 (2007).
- ⁴²S. Gonchenko, D. Turaev, and L. Shilnikov, “Homoclinic tangencies of arbitrarily high orders in the Newhouse regions,” *J. Math. Sci.* **105**, 1738–1778 (2001).
- ⁴³S. V. Gonchenko, I. Ovsyannikov, C. Simó, and D. Turaev, “Three-dimensional Hénon-like maps and wild Lorenz-like attractors,” *Int. J. Bifurcat. Chaos* **15**, 3493–3508 (2005).
- ⁴⁴S. V. Gonchenko, A. S. Gonchenko, and L. P. Shilnikov, “Towards scenarios of chaos appearance in three-dimensional maps,” *Rus. J. Nonlin. Dyn.* **8**, 3–28 (2012).
- ⁴⁵S. Gonchenko, A. Gonchenko, I. Ovsyannikov, and D. Turaev, “Examples of Lorenz-like attractors in Hénon-like maps,” *Math. Model. Nat. Phenom.* **8**, 48–70 (2013).
- ⁴⁶A. Gonchenko and S. Gonchenko, “Variety of strange pseudohyperbolic attractors in three-dimensional generalized Hénon maps,” *Phys. D: Nonlinear Phenom.* **337**, 43–57 (2016).
- ⁴⁷F. Takens, “Unfoldings of certain singularities of vectorfields: Generalized Hopf bifurcations,” *J. Differ. Equ.* **14**, 476–493 (1973).
- ⁴⁸V. I. Arnold, *Geometrical Methods in the Theory of Ordinary Differential Equations* (Springer Science & Business Media, 2012), Vol. 250.
- ⁴⁹L. P. Shilnikov, A. Shilnikov, D. Turaev, and L. Chua, *Methods of Qualitative Theory in Nonlinear Dynamics. Parts I and II*, World Scientific Series on Nonlinear Science Series A (World Scientific, 1998, 2001), Vol. 5.
- ⁵⁰A. L. Shilnikov, L. P. Shilnikov, and D. Turaev, “Normal forms and Lorenz attractors,” *Int. J. Bifurcat. Chaos* **3**, 1123–1139 (1993).
- ⁵¹A. Shilnikov, “Bifurcations and chaos in the Shimizu–Morioka system,” in *Methods and Qualitative Theory of Differential Equations* (Gorky State University, 1986), pp. 180–193.
- ⁵²A. Shilnikov, “Bifurcations and chaos in the Shimizu–Morioka system: II,” in *Methods and Qualitative Theory of Differential Equations* (Gorky State University, 1989), pp. 130–137.
- ⁵³A. Shilnikov, “Bifurcation and chaos in the Morioka–Shimizu system,” *Sel. Math. Sov.* **10**, 105–117 (1991).
- ⁵⁴A. Gonchenko, S. Gonchenko, A. Kazakov, and D. Turaev, “Simple scenarios of onset of chaos in three-dimensional maps,” *Int. J. Bifurcat. Chaos* **24**, 1440005 (2014).
- ⁵⁵A. A. Simonov, “The investigation of piecewise monotone transformations of an interval by the methods of symbolic dynamics,” *Dokl. Akad. Nauk* **238**, 1063–1066 (1978).
- ⁵⁶V. S. Afraimovich, V. Bykov, and L. P. Shilnikov, “Attractive nonrough limit sets of Lorenz-attractor type,” *Tr. Mosk. Mat. Obs.* **44**, 150–212 (1982).
- ⁵⁷A. L. Shilnikov, “On bifurcations of the Lorenz attractor in the Shimizu–Morioka model,” *Phys. D: Nonlinear Phenom.* **62**, 338–346 (1993).
- ⁵⁸Y. A. Kuznetsov, *A Tutorial for MatContM GUI* (Utrecht University, Utrecht, 2013).
- ⁵⁹H. Meijer, W. Govaerts, Y. A. Kuznetsov, R. K. Ghaziani, and N. Neiryneck, “MatContM: A toolbox for continuation and bifurcation of cycles of maps: Command line use,” (Department of Mathematics, Utrecht University, 2017).
- ⁶⁰H. G. E. Meijer, W. Govaerts, Yu. A. Kuznetsov, R. Khoshshar, Ghaziani, and N. Neiryneck, “MatContM: Numerical bifurcation analysis toolbox in MATLAB,” (Department of Mathematics, Utrecht University, 2020).
- ⁶¹G. Benettin, L. Galgani, A. Giorgilli, and J.-M. Strelcyn, “Lyapunov characteristic exponents for smooth dynamical systems and for Hamiltonian systems; a method for computing all of them. Part 1: Theory,” *Meccanica* **15**, 9–20 (1980).
- ⁶²A. Chenciner, “Bifurcations de points fixes elliptiques-I. Courbes invariantes,” *Publ. Math. IHÉS* **61**, 67–127 (1985).
- ⁶³Y. A. Kuznetsov, H. G. Meijer, and L. van Veen, “The fold-flip bifurcation,” *Int. J. Bifurcat. Chaos* **14**, 2253–2282 (2004).
- ⁶⁴N. Gavrilov, “On some bifurcations of an equilibrium with two pairs of pure imaginary roots,” *Methods Qual. Theory Differ. Equ.* **1**, 17–30 (1980).
- ⁶⁵Y. A. Kuznetsov, *Elements of Applied Bifurcation Theory* (Springer, 1998), Vol. 112.
- ⁶⁶S. Gonchenko, M. Kainov, A. Kazakov, and D. Turaev, “On methods for verification of the pseudohyperbolicity of strange attractors,” *Izv. VUZ. Appl. Nonlinear Dyn.* **29**, 160–185 (2021).
- ⁶⁷P. V. Kuptsov and S. P. Kuznetsov, “Lyapunov analysis of strange pseudohyperbolic attractors: Angles between tangent subspaces, local volume expansion and contraction,” *Regul. Chaotic Dyn.* **23**, 908–932 (2018).
- ⁶⁸P. V. Kuptsov, “Fast numerical test of hyperbolic chaos,” *Phys. Rev. E* **85**, 015203 (2012).
- ⁶⁹P. V. Kuptsov and U. Parlitz, “Theory and computation of covariant Lyapunov vectors,” *J. Nonlinear Sci.* **22**, 727–762 (2012).
- ⁷⁰V. Afraimovich and L. Shilnikov, “Strange attractors and quasiattractors,” in *Nonlinear Dynamics and Turbulence*, edited by G. I. Barenblatt, G. Iooss, and D. D. Joseph (Pitman Advanced Publishing Program, 1983).
- ⁷¹Z. Galias and P. Zgliczyński, “Computer assisted proof of chaos in the Lorenz equations,” *Phys. D: Nonlinear Phenom.* **115**, 165–188 (1998).
- ⁷²W. Tucker, “A rigorous ODE solver and Smale’s 14th problem,” *Found. Comput. Math.* **2**, 53–117 (2002).
- ⁷³M. J. Capiński and A. Wasieczko-Zajac, “Computer-assisted proof of Shilnikov homoclinics: With application to the Lorenz-84 model,” *SIAM J. Appl. Dyn. Syst.* **16**, 1453–1473 (2017).
- ⁷⁴M. J. Capiński, D. Turaev, and P. Zgliczyński, “Computer assisted proof of the existence of the Lorenz attractor in the Shimizu–Morioka system,” *Nonlinearity* **31**, 5410 (2018).
- ⁷⁵S. Képley and J. M. James, “Chaotic motions in the restricted four body problem via Devaney’s saddle-focus homoclinic tangle theorem,” *J. Differ. Equ.* **266**, 1709–1755 (2019).